A Self-Reinforcing Neuroimmune Clearance–Pruning Loop and Its EEG Signature: A Spatially Graded Hypothesis for Autism Spectrum Disorder and Developmental Dyslexia, A Perspective

Günet Eroğlu

Department of Computer Engineering, Faculty of Engineering and Natural Sciences, Bahçeşehir University, Istanbul, Turkey

Corresponding author: gunet.eroglu@healthmobilesoftware.com

Abstract. Autism spectrum disorder (ASD) and developmental dyslexia share a common low-frequency (theta-range) EEG shift, yet differ systematically in its spatial extent — diffuse in ASD, left-temporoparietal and focal in dyslexia. This conjunction — a shared, direction-invariant low-frequency signature co-occurring with a systematic spatial dissociation — is the single observation this framework is built to explain, and no existing account, I argue, predicts it as a unit. I propose that it arises from a self-reinforcing loop between two systems usually studied apart: microglial synaptic pruning and the brain's glymphatic–meningeal lymphatic clearance. Each drives the other — reactive microglia raise the clearance burden, and impaired clearance sustains the inflammatory tone that keeps microglia reactive — so the pair behaves as one bistable system whose clinical expression is set by two parameters: the *direction* of pruning error and its *spatial extent*. I support the proposal with a cause-and-effect molecular pathway (AQP4–cytokine–C1q/C3/CR3/C4b–CX3CR1), a biophysical account of *why theta specifically* (thalamocortical dysrhythmia from reduced recurrent excitation), a region-specific rationale for left-temporoparietal vulnerability in dyslexia, and a network-level EEG framework (connectivity, graph topology, phase-locking, entropy, microstates, cross-frequency coupling, source localization) rather than power alone. The chain is formalized as a compact dynamical model exhibiting bistability and hysteresis, and yields falsifiable predictions with an explicit falsification experiment. Evidence remains largely correlational and preclinical; the aim is a testable organizing framework, not a proven mechanism. The novelty lies in the *coupling* — treating pruning and clearance as one bistable system — not in any individual mechanism, and the framework is deliberately bounded: it aims to explain one EEG conjunction across two disorders, not either disorder in full.

Keywords: autism spectrum disorder; dyslexia; glymphatic/meningeal lymphatic system; microglial pruning; thalamocortical dysrhythmia; EEG network biomarkers.

1. Introduction: two literatures that belong together

Circuit maturation depends on microglia removing weak or redundant synapses (Paolicelli & Ferretti, 2017) and on the glymphatic and meningeal lymphatic pathways clearing metabolic and immune debris (Iliff & Nedergaard, 2013), yet the two are almost always

Received date: July 21 2026
Revised dates;July 22,July 27, Aug,9
Accepted date: Aug. 9 2026

DOI: https://10.63211/j.p.26.204502
ISSN 2760-8646 (Online) ICAITD

treated as separate programs. That separation is, I argue, an artifact of disciplinary boundaries: activated microglia release cytokines and reactive species that add to the waste load, and impaired clearance prolongs the inflammatory milieu that biases microglia toward reactive, pruning-altering states (Rasmussen, Mestre, & Nedergaard, 2018; Meng, Zhang, & Zhang, 2024). Recent pediatric imaging makes the coupling concrete: diffusion-based glymphatic indices (DTI-ALPS) are reduced in children with ASD and ADHD and track sleep quality and language delay (Abnormal glymphatic function in ASD, 2025; Impaired glymphatic function in ADHD, 2025).

My central claim is that this loop has a macroscopic read-out. Because EEG integrates the activity of large synaptic populations, a shift in the balance between synaptic elimination and preservation should appear as reproducible changes in oscillatory power, coordination, and network topology. If so, the recurrent EEG abnormalities of ASD and dyslexia are not two unrelated findings but one loop expressed in two spatial regimes.

2. The hypothesis, and why these two disorders

Formally: *(i)* reduced glymphatic/meningeal clearance elevates and prolongs regional neuroinflammation; *(ii)* this shifts microglia toward states that over- or under-prune; *(iii)* the altered synaptic drive perturbs cortical rhythm generation; and *(iv)* the net effect is a low-to-high frequency power shift with degraded network coordination (Fig. 1). Two parameters govern phenotype, and they act asymmetrically by design. The low-frequency (theta) shift is the *convergent* output both pruning directions share (Section 4), so it is what ASD and dyslexia have in common; *direction* of pruning error then sets connectivity topology (hypo- versus hyper-connectivity), while *spatial extent* sets the layout of both the spectral and the connectivity abnormality (diffuse versus focal). One convergent signature and two differentiating axes — not two interchangeable parameters — is the intended logical structure.

Why ASD and dyslexia rather than ADHD, schizophrenia, or epilepsy? The pair is a minimal, maximally informative contrast. Both are childhood-onset neurodevelopmental conditions whose symptoms emerge during the peak window of synaptic pruning and clearance-system maturation, so the loop is developmentally "on" when the phenotype forms. Crucially, they bracket the spatial axis the model predicts: ASD shows distributed connectivity differences and a broad power shift, whereas dyslexia shows a focal, task-locked left-temporoparietal signature with otherwise typical global connectivity (Gabrieli, 2009). Testing one diffuse and one focal disorder is the sharpest available test of the spatial-extent claim. Schizophrenia (later onset, dominated by complement-driven over-elimination) and epilepsy (primary hyperexcitability) are better framed as later extensions; ADHD, where DTI-ALPS is already reduced and correlates with clinical scores, is the most natural next test and is treated as a prediction below.

Received date: July 21 2026
Revised dates;July 22,July 27, Aug,9
Accepted date: Aug. 9 2026

DOI: https://10.63211/j.p.26.204502
ISSN 2760-8646 (Online) ICAITD

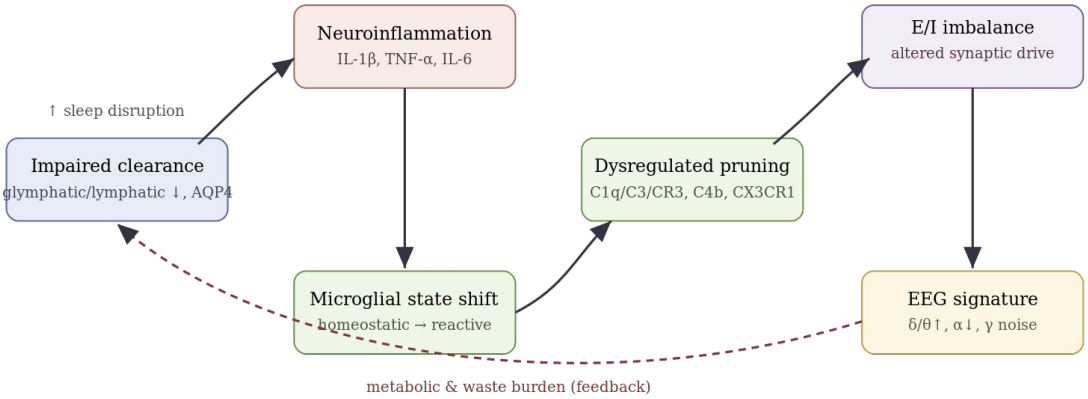

Figure 1. The self-reinforcing clearance–pruning loop. Reduced clearance (AQP4 depolarization, glymphatic/meningeal drainage) raises neuroinflammatory tone, shifting microglia toward reactive states that mis-tune complement- and fractalkine-dependent pruning; the resulting excitation/inhibition (E/I) imbalance perturbs rhythm generation, producing the EEG signature. The dashed arrow marks the feedback by which inflammatory and metabolic byproducts further tax clearance. Sleep disruption is an external modulator that lowers clearance efficiency.

A caveat on heterogeneity. Calling ASD "diffuse" is a statement about central tendency, not uniformity. Connectivity studies partition ASD into hypo-connected, hyper-connected, and near-normal subgroups, and the same child can show both directions in different systems. The model accommodates this directly: the *direction* parameter and the predicted cortical mosaic make ASD not a single point but a *distribution* weighted toward spatially extensive involvement, whereas dyslexia is weighted toward a focal left-temporoparietal locus. The claim is thus probabilistic and subtype-aware — a difference in the spatial *spread* of pruning error, not a categorical assignment of every case — and any test of it must be stratified by connectivity subtype rather than by diagnosis alone.

3. The molecular pathway (cause and effect)

The loop is only as strong as its molecular links, so I make them explicit (Fig. 2). On the clearance side, aquaporin-4 (AQP4) at astrocytic endfeet governs perivascular water and solute exchange; cytokines from reactive microglia rapidly depolarize AQP4 localization, and loss of AQP4 polarity impairs clearance while amplifying astrocytic cytokine release — a bidirectional microglia–AQP4 coupling that ties inflammation to clearance failure (AQP4 fluidic connectome, 2025). Reduced drainage prolongs exposure to IL-1β, TNF-α, and IL-6, the cytokines repeatedly reported in ASD and learning-disability cohorts (Estes & McAllister, 2015; EEG-based neuroinflammation in learning disabilities, 2025).

On the effector side, cytokine tone determines *which way* pruning fails. Excess complement activation drives over-elimination: C1q tags synapses, C3 fragments are deposited, and CR3-bearing microglia engulf them. This arm is causally engaged in ASD models — SCN2A deficiency produces microglial over-pruning in mice and human organoids (SCN2A over-pruning, 2024), and elevated neuronal C4b (downstream of the risk gene SETDB1 and of

Received date: July 21 2026
Revised dates;July 22,July 27, Aug,9
Accepted date: Aug. 9 2026

DOI: https://10.63211/j.p.26.204502
ISSN 2760-8646 (Online) ICAITD

maternal immune activation) triggers excessive prefrontal pruning and autistic-like behavior (C4b/SETDB1, 2026). The opposing arm is under-pruning: deficient CX3CL1–CX3CR1 (fractalkine) signaling delays synapse elimination and maturation. Crucially, the retained synapses are not added excitatory drive: in the fractalkine-deficient brain the anatomical surplus coexists with delayed maturation, weak transmission, and *reduced* long-range connectivity (Zhan et al., 2014) — a distinction that becomes decisive for the spectral prediction in Section 4. TREM2–DAP12 and modulators such as vitamin D receptor signaling set the microglial set-point between these arms. The model therefore predicts that *complement-biased* states yield frank hypoconnectivity, while *fractalkine-biased* states yield *local, anatomical* hyperconnectivity superimposed on *reduced effective and long-range* drive, with real cortex showing a spatial mosaic of both. Both arms converge on reduced *effective* recurrent drive into the thalamocortical loop — over-pruning by removing excitatory synapses outright, under-pruning by leaving weak, immature ones that fail to deliver reliable drive.

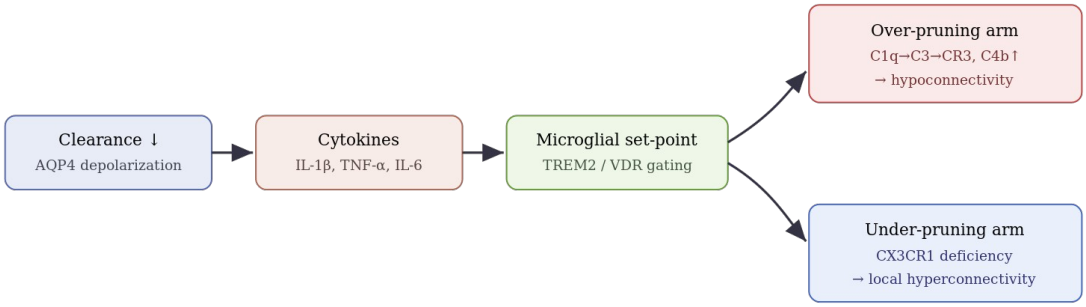

Figure 2. Cause-and-effect molecular pathway. Clearance failure and AQP4 depolarization raise cytokine tone, which sets the microglial state (gated by TREM2 and vitamin D receptor signaling). Depending on that set-point, the complement arm (C1q/C3/CR3, neuronal C4b) over-prunes toward hypoconnectivity, or the fractalkine arm (CX3CR1) under-prunes toward local hyperconnectivity. Real cortex is predicted to show a spatial mosaic of both.

The arrows in Figure 2 do not carry equal evidential weight, so I grade each link explicitly. *Established in humans:* altered glymphatic/clearance indices in ASD (DTI-ALPS) and the association of complement genes (e.g. C4) with neurodevelopmental risk. *Supported preclinically but not yet confirmed developmentally in humans:* AQP4–dependent clearance, cytokine control of microglial state, complement-mediated (C1q/C3/CR3) synapse elimination, and CX3CR1-dependent pruning, each resting largely on rodent work. *Inferred / not yet directly tested:* the coupling between a given microglial set-point and the *direction* of pruning error in humans, and the proposed cortical mosaic. Figure 2 is thus a hypothesis about how independently attested mechanisms could be wired together, not a claim that the full pathway has been demonstrated end to end; its weakest links — the direction-setting step and the mosaic — are precisely those the experiments in Section 9 target.

Received date: July 21 2026
Revised dates;July 22,July 27, Aug,9
Accepted date: Aug. 9 2026

DOI: https://10.63211/j.p.26.204502
ISSN 2760-8646 (Online) ICAITD

3.1 Where does the bias come from, and how central is AQP4?

The framework's weakest-specified step is also its most important: what tips a given cortical region toward the complement (over-pruning) versus the fractalkine (under-pruning) arm? I do not claim to know, but the candidate sources are enumerable, each with a different testable prediction. *Genetic:* common and rare variation in complement genes (notably *C4* copy number) and in *CX3CR1* would bias the set-point constitutively, predicting heritable, bilateral tendencies. *Environmental / immune:* maternal immune activation, early-life infection, or chronic inflammatory load would push it toward the complement arm in a dose- and timing-dependent way, predicting associations with prenatal exposures rather than genotype. *Epigenetic:* activity-dependent methylation of complement and fractalkine regulators could explain why a use-dependent region such as left temporoparietal cortex is preferentially affected in dyslexia — a regional, experience-gated bias. *Stochastic:* developmental noise near the bistable threshold (Section 7.1) could produce mosaic, idiosyncratic patterns with low recurrence in relatives. These are not mutually exclusive, and distinguishing them is itself a program: genetic and prenatal-exposure biasing predict diffuse involvement (the ASD-weighted pole), whereas experience-gated epigenetic biasing predicts the focal, lateralized pole. Making the origin of the bias explicit — rather than treating "complement-biased" as a primitive — is the single change that would most strengthen the mechanistic core.

AQP4 is one node, not the regulator. Figure 2 foregrounds AQP4 for concreteness, but clearance is multifactorial and the model should not be read as AQP4-centric. Meningeal lymphatic drainage, perivascular (glymphatic) flow, arterial pulsatility, sleep and slow-wave activity, astrocytic volume regulation, and venous/CSF egress all contribute; AQP4 polarization is best understood as one measurable proxy for this larger system rather than its master switch. The hypothesis needs only that *effective* clearance falls — which upstream factor dominates likely varies by individual and stage — and the imaging read-outs proposed (DTI-ALPS, dynamic-contrast MRI, NIRS) deliberately index the aggregate, not AQP4 alone.

4. Why *theta* specifically: a biophysical bridge

Why should the loop elevate theta rather than beta? Because reduced *effective* recurrent excitation — the convergent consequence of *both* pruning directions (over-pruning removes excitatory synapses directly; under-pruning leaves immature, weak ones that likewise fail to deliver reliable drive), compounded by inflammatory suppression of excitatory transmission — deafferents thalamocortical circuits, the classic trigger for *thalamocortical dysrhythmia*. Deprived of excitatory drive, thalamic relay neurons hyperpolarize, de-inactivate T-type Ca^{2+} channels, and switch from tonic to low-threshold burst firing in the delta–theta range; corticothalamic feedback then entrains cortex to this slow rhythm (Llinás et al., 1999). The same mechanism predicts the rest of the signature: reduced lateral inhibition at the "edges" of the slowed domain releases high-frequency *gamma* as cortical "noise," while *alpha* — dependent on intact thalamo-cortico-thalamic feedback and precise interneuron timing — is degraded. Beta, tied more to sensorimotor and cortico–basal-ganglia loops, is comparatively spared because the primary lesion is relay-mode switching, not beta-generating circuitry. The observed profile (δ/θ↑, α↓, γ

Received date: July 21 2026
Revised dates;July 22,July 27, Aug,9
Accepted date: Aug. 9 2026

DOI: https://10.63211/j.p.26.204502
ISSN 2760-8646 (Online) ICAITD

noise, relative beta stability) is thus not a list of coincidences but the coherent output of one mechanism (Fig. 3); AQP4-linked disturbance of extracellular K^+ and osmotic buffering provides a second, convergent route to the same excitability shift.

Two clarifications guard against misreading. First, because both pruning directions converge on reduced effective drive, the theta shift is *direction-invariant*: the two arms share it, while connectivity topology — not the spectral shift — distinguishes them (Section 7), so one loop predicts a common spectral change alongside opposite connectivity outcomes. Second, this theta is the *persistent, waking* rhythm of thalamocortical dysrhythmia (Llinás et al., 1999), distinct from the ordinary theta slowing of drowsiness. The two resemble each other in a raw spectrum, so the prediction is specific: TCD-type theta should appear during alert task performance and persist independent of arousal. Recordings must therefore control vigilance — via simultaneous arousal monitoring and alert-task paradigms — so a trait signature is not confounded by a state one. A drowsiness account is not an alternative but a confound the design must exclude.

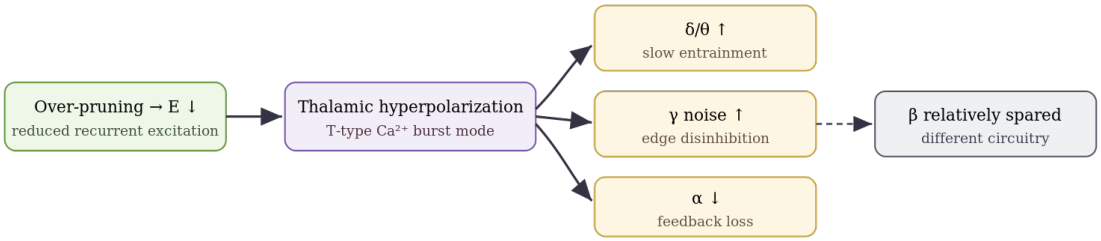

Figure 3. Biophysical account of the spectral signature via thalamocortical dysrhythmia. Reduced recurrent excitation hyperpolarizes thalamic relay neurons into T-type Ca^{2+} burst firing, entraining cortex to δ/θ; edge disinhibition releases γ "noise"; loss of thalamo-cortico-thalamic feedback lowers α. β, generated by partly separate circuitry, is comparatively spared — explaining *why theta, not beta*.

5. Left-temporoparietal vulnerability in dyslexia

Why should the loop strike the left temporoparietal cortex in dyslexia? Three region-specific factors converge. First, left perisylvian language cortex is among the latest-maturing and most protractedly myelinated regions, so it spends longer in the pruning-and-clearance-sensitive window during the very years reading is acquired. Second, learning to read imposes a steep, regionally concentrated metabolic and plasticity demand on this circuit, raising local waste production and clearance dependence. Third, perivascular and drainage architecture is not uniform, so a region under peak load is disproportionately exposed when clearance efficiency dips (e.g., with the sleep disruption common in these children). Under the model, a spatially confined loop here yields the reported focal signature — increased left-temporoparietal and frontal-midline theta with reduced upper-alpha suppression during reading, and atypical delta–theta phase–amplitude coupling — while sparing global connectivity (Larrain-Valenzuela et al., 2017; Developmental dyslexia EEG and molecular signatures, 2024). Peripheral IL-6/TNF-α elevations reported in subsets of children with learning disabilities are consistent, though

Received date: July 21 2026
Revised dates;July 22,July 27, Aug,9
Accepted date: Aug. 9 2026

DOI: https://10.63211/j.p.26.204502
ISSN 2760-8646 (Online) ICAITD

central microglial evidence in dyslexia is still absent and is the key missing test (EEG-based neuroinflammation in learning disabilities, 2025).

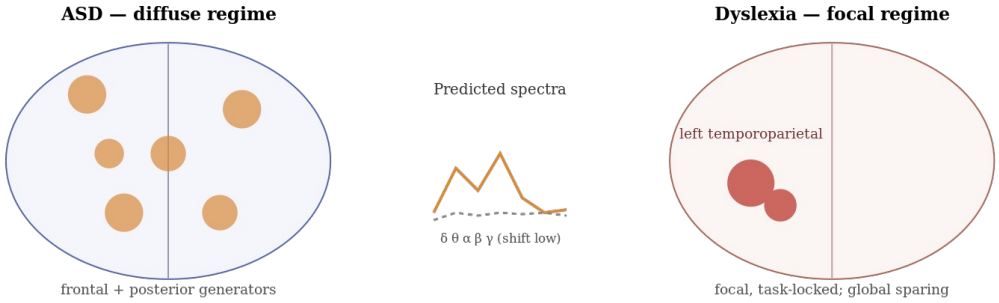

Figure 4. One loop, two spatial regimes. Uniform perturbation of clearance/inflammation reproduces the distributed ASD signature (multiple frontal and posterior generators, broad low-frequency shift); a left-temporoparietal perturbation reproduces the focal, task-locked dyslexia signature with relative global sparing. Center: predicted spectral mass shift toward low frequencies (solid = affected, dashed = typical).

6. EEG as a network read-out, not a power spectrum

Power alone is too blunt to carry the hypothesis, so the model should be evaluated against multi-domain EEG features (Table 1). *Functional connectivity* in young children with ASD shows coexisting hypo- and hyper-connectivity — exactly the mosaic the two pruning arms predict (Multidimensional connectivity in preschool ASD, 2026). *Graph-theoretic topology* (reduced global efficiency, altered modularity and small-worldness) indexes the network cost of mis-tuned pruning and now supports ASD classification (Dynamic local graph-theory EEG, 2024). *Phase-locking* and *cross-frequency (alpha–gamma, delta–theta) coupling* capture the coordination failures the dysrhythmia model predicts (Berman et al., 2016). *Entropy/complexity* and *EEG microstates* add temporal-dynamics fingerprints that discriminate ASD (Explainable-AI microstates in ASD, 2026; Bosl et al., 2011). *Source localization* lets the framework test its central spatial claim — diffuse generators in ASD versus a left-temporoparietal focus in dyslexia. The prediction is concrete: the two disorders should differ less in *which* features are abnormal than in the *spatial layout* of those abnormalities.

Two clarifications the analysis demands. First, *why prioritize graph topology and microstates?* Because they most directly index the quantity the model constrains — the *organization* of network drive rather than local power: global efficiency and modularity read out the integration cost of mis-tuned pruning, and microstate syntax reads out the temporal stability of coordination that thalamocortical dysrhythmia should disturb. Phase–amplitude coupling, entropy, and raw connectivity are informative but sit further downstream and are more confound-prone, so Section 9 designates them confirmatory. Second, the static, single-feature framing undersells what is now possible: dynamic functional connectivity and hidden Markov models can test the *bistability/hysteresis* prediction directly (dwell times in pathological network states), neural-mass and whole-brain models can turn the §7.1 loop into a spatially explicit generator of the predicted spectra, and graph-neural-network classifiers can test whether the diffuse-versus-focal

Received date: July 21 2026
Revised dates;July 22,July 27, Aug,9
Accepted date: Aug. 9 2026

DOI: https://10.63211/j.p.26.204502
ISSN 2760-8646 (Online) ICAITD

contrast, rather than any single band, carries the diagnostic information. These methods bridge the compact model to data.

Table 1. *Multi-domain EEG features the model must explain, and its predictions.*

Feature domain	ASD (diffuse regime)	Dyslexia (focal regime)	Loop interpretation
Spectral power	δ/θ↑ broad; α↓; γ noise↑	θ↑ left TP + frontal midline; upper-α↓	Thalamocortical dysrhythmia from reduced drive
Functional connectivity	Coexisting hypo- and hyper-connectivity	Reduced left-hemisphere language coupling	Complement vs fractalkine pruning mosaic
Graph topology	↓ global efficiency, altered modularity	Local inefficiency, near-normal global	Network cost of mis-tuned pruning
Cross-frequency coupling	Disrupted α–γ PAC	Atypical δ–θ PAC in reading	Loss of E/I-dependent nesting
Microstates / entropy	Altered dynamics & complexity	Task-locked microstate anomalies	Temporal instability of coordination
Source localization	Distributed generators	Left-temporoparietal focus	Spatial extent of the active loop

7. A compact systems model

The verbal chain can be written as a minimal set of coupled relations, intended as a conceptual scaffold for a fuller computational model rather than a fitted equation. Let clearance efficiency C, inflammatory tone N, microglial reactivity M, pruning error P (signed: positive = over-pruning), and the excitation/inhibition ratio E evolve so that N rises as C falls, M rises with N, and P is set by M and its molecular bias b (complement vs fractalkine):

$$N \propto 1/C \;\cdot\; M = f(N, \text{TREM2}, \text{VDR}) \;\cdot\; P = b \cdot M \;\cdot\; E \downarrow \text{ as } |P| \uparrow \;\cdot\; C \downarrow \text{ as } N \uparrow \text{ (feedback)}$$

A structural feature of this scheme carries the paper's logic: E falls with $|P|$, the *magnitude* of pruning error, not its sign. Any sufficient deviation from optimal pruning — over- or under-pruning — reduces effective recurrent drive, which is why the theta shift is direction-invariant; the *sign* of P (the molecular bias b) sets only whether connectivity is pushed toward the hypo- or hyper-connective pole. The model thus encodes the "one convergent signature, two differentiating axes" structure of Section 2 directly, with low E driving the relay-mode switch that shifts spectral mass toward δ/θ and releases edge gamma (Section 4). The feedback term (C falls as N rises) makes the system self-reinforcing and bistable: past a threshold it settles into a chronic low-C/high-N attractor, which may be why the EEG phenotype is stable rather than transient. Letting C, N, and b vary by region turns a uniform perturbation into the ASD regime and a left-temporoparietal one into the dyslexia regime — the object a future neural-mass simulation should instantiate.

Received date: July 21 2026
Revised dates;July 22,July 27, Aug,9
Accepted date: Aug. 9 2026

DOI: https://10.63211/j.p.26.204502
ISSN 2760-8646 (Online) ICAITD

7.1 A dynamical simulation of the loop

To move from a verbal to a computational hypothesis, I instantiate the feedback as two coupled ordinary differential equations in which clearance efficiency C and inflammatory tone N mutually repress one another with cooperativity (Hill coefficient $h = 4$):

$$dC/dt = \varepsilon_C [\ \sigma \cdot K_c^h/(K_c^h+N^h) - C\ ] \quad \cdot \quad dN/dt = \varepsilon_N [\ \rho \cdot K_i^h/(K_i^h+C^h) + n_0 - N\ ]$$

Microglial reactivity $M(N)$, effective recurrent drive E, and relative theta power $\theta(E)$ are read out algebraically from the state. With biologically plausible parameters the system is *bistable*: a healthy state and a pathological low-C/high-N state are separated by an unstable saddle that acts as a threshold (Fig. 5A) — the formal counterpart of the loop's self-reinforcing character. The immediate consequence is *hysteresis* (Fig. 5B): a sub-threshold clearance insult decays and the system returns to health, whereas an otherwise identical supra-threshold insult tips it across the separatrix, after which the theta elevation *persists once the insult is gone*. This gives a concrete reason the EEG phenotype is developmentally stable rather than transient, and why perturbations during the pruning window could leave lasting electrophysiological traces; letting C, N, and the molecular bias b vary by region reproduces the diffuse (ASD) and focal (dyslexia) regimes within the same equations. I adopt this as a *phenomenological* rather than mechanistically derived model: the Hill terms and $h = 4$ are chosen to capture the switch-like, cooperative character of microglial and clearance dynamics, not to fit molecular rate constants. Its value is qualitative — it shows that a loop of this *form* can generate bistability and hysteresis — so the claims that follow concern the topology of the dynamics, not specific parameter values, and those qualitative predictions are themselves falsifiable.

Why this topology, and not another? The parameter values matter less than the *structure* of the model, so I make that choice explicit. The essential ingredient is *mutual repression with cooperativity*: clearance and inflammatory tone each suppress the other with a threshold-like (Hill) response. This is the minimal motif that generates bistability, and it mirrors the one biological fact the paper rests on — that the two processes drive each other in opposite directions. Alternative topologies make different predictions: a *mutual-activation* loop is also bistable but predicts co-elevation rather than the observed anti-correlation of clearance and inflammation; a single self-inhibiting node with delay predicts oscillation rather than a sustained shifted state; and a linear, non-cooperative coupling predicts a graded, fully reversible response with no threshold or hysteresis. These alternatives are discriminable: the bistable, hysteretic, anti-correlated regime assumed here predicts a *persistent* post-insult state and a recovery threshold (Fig. 6), which the oscillatory and linear alternatives do not. The topology is thus not arbitrary but the simplest one consistent with the anti-correlation and developmental persistence the framework must explain — and it is falsifiable at the level of structure, not just parameters.

Received date: July 21 2026
Revised dates;July 22,July 27, Aug,9
Accepted date: Aug. 9 2026

DOI: https://10.63211/j.p.26.204502
ISSN 2760-8646 (Online) ICAITD

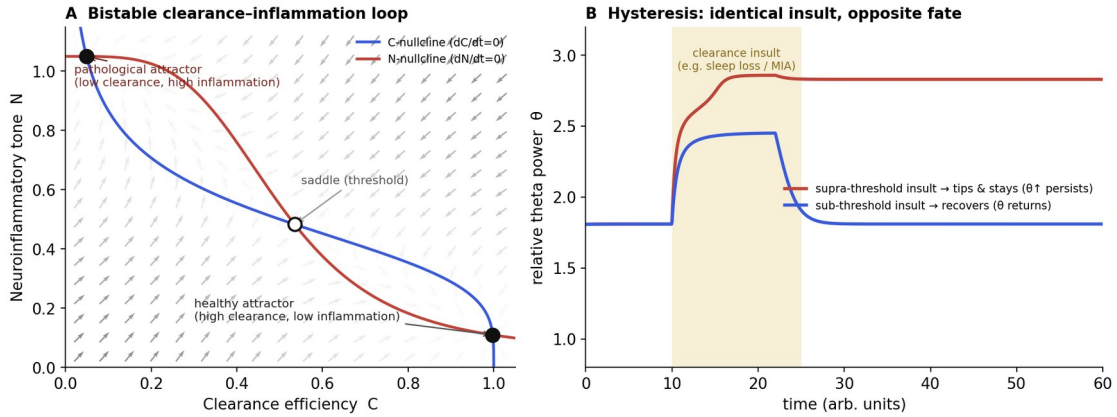

Figure 5. Computational instantiation of the loop as two coupled ordinary differential equations (clearance C, inflammatory tone N; mutual repression with Hill coefficient 4). *(A)* Phase plane: the two nullclines intersect at two *stable* attractors — a healthy state (high C, low N, low theta) and a pathological state (low C, high N, elevated theta) — separated by an unstable saddle that sets a threshold, formalizing the self-reinforcing loop as a bistable system. *(B)* Hysteresis: a transient clearance insult (shaded; e.g., sleep loss or immune activation) that stays below threshold decays and theta returns to baseline (blue), whereas an identical-form but supra-threshold insult tips the system across the separatrix into the chronic attractor, where the theta elevation *persists after the insult ends* (red). This gives a concrete, falsifiable reason the EEG phenotype is developmentally stable rather than transient.

A phenomenological model earns trust only if its central behaviour is not an artefact of one lucky parameter set, so I characterized the dynamics quantitatively (Fig. 6). Treating a sustained inflammatory drive μ as a slow control parameter reveals a classic *saddle-node (fold) bifurcation* with an explicit hysteresis loop: the healthy branch loses stability at an upper fold ($\mu \approx 0.17$), while recovery requires driving μ back down to a distinct lower fold ($\mu \approx -0.11$), so the system does not retrace its path (Fig. 6A). The width of this bistable window measures how strongly the disorder resists reversal. A sweep over the cooperativity h (Fig. 6B) shows the result is robust: bistability is absent for $h \lesssim 2.3$ and widens monotonically for $h \gtrsim 3$, so $h = 4$ sits inside the switch-like regime rather than on a knife-edge. Finally, a two-parameter regime map over the clearance and inflammatory drives (σ, ρ) partitions the plane into monostable-healthy, monostable-pathological, and intervening bistable bands, with the physiological baseline near the healthy edge of that band — exactly the vulnerable configuration a self-reinforcing hypothesis requires (Fig. 6C). These analyses turn the phase-plane illustration into a dynamical result: the qualitative predictions survive parameter variation, and the boundaries of the bistable region are themselves quantitative, testable targets.

Received date: July 21 2026
Revised dates;July 22,July 27, Aug,9
Accepted date: Aug. 9 2026

DOI: https://10.63211/j.p.26.204502
ISSN 2760-8646 (Online) ICAITD

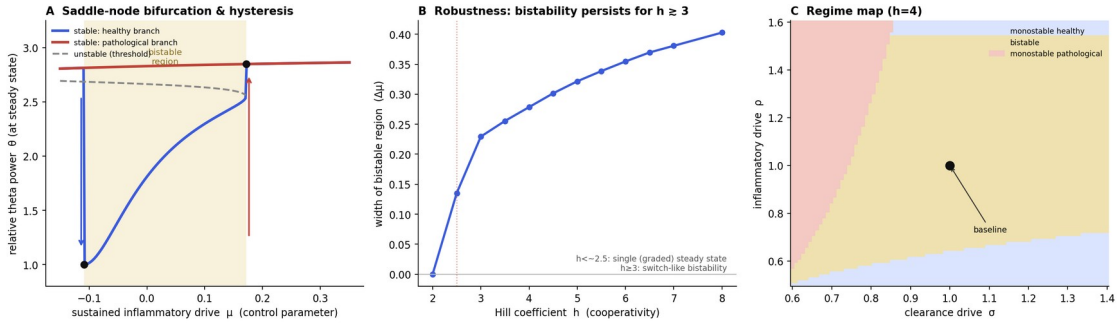

Figure 6. Quantitative analysis of the loop dynamics. *(A)* Bifurcation diagram: steady-state theta power versus a sustained inflammatory drive μ. Solid blue and red curves are stable branches (healthy, pathological); the dashed grey curve is the unstable threshold. The two fold points bound a bistable region (shaded); arrows trace the hysteresis loop, so tipping up and recovering occur at different values of μ. *(B)* Robustness: the width of the bistable region as a function of the Hill coefficient h. Bistability is absent below $h \approx 2.3$ and grows smoothly thereafter, showing the switch-like behaviour is not a fine-tuned artefact. *(C)* Two-parameter regime map ($h = 4$) over clearance drive σ and inflammatory drive ρ: monostable-healthy (blue), bistable (yellow), and monostable-pathological (red) regions. The baseline operating point lies near the healthy edge of the bistable band.

8. Relation to existing frameworks

The model borrows pieces from several established theories; its novelty lies in how it couples them (Table 2). The contribution is not a new molecule or rhythm but a *bidirectional, bistable coupling* that turns five partial accounts into one developmental loop with a shared EEG output and a spatial axis.

Table 2. *How the proposed loop relates to existing frameworks.*

Framework	Core claim	Primary scope	Relation to the present model
E/I imbalance (Rubenstein & Merzenich, 2003)	Elevated cortical excitation/inhibition ratio underlies ASD	ASD	Treated as a *downstream node*, not the prime cause; the loop supplies the upstream clearance–inflammation driver and predicts the E/I sign can differ by region (over- vs under-pruning)
Thalamocortical dysrhythmia (Llinás et al., 1999)	Deafferentation switches thalamus to burst firing, producing persistent low-frequency	Pain, tinnitus, neuropsychiatric	Adopted as the biophysical *output stage*; the model adds a developmental neuroimmune *cause*

Received date: July 21 2026
Revised dates;July 22,July 27, Aug,9
Accepted date: Aug. 9 2026

DOI: https://10.63211/j.p.26.204502
ISSN 2760-8646 (Online) ICAITD

	rhythm		for the reduced drive and ties it to a diffuse-vs-focal spatial axis
Complement / microglial over-pruning (Sekar et al., 2016; ASD pruning models)	Excess complement-tagged synapse elimination	Schizophrenia, ASD	Incorporated as *one arm*; the model adds the opposing under-pruning arm and the clearance feedback, and derives a shared spectral output
Glymphatic / clearance dysfunction (Nedergaard and colleagues)	Impaired waste clearance drives neural disease	Ageing, Alzheimer's, sleep	Elevated from a largely degenerative idea to a *developmental driver* coupled bidirectionally to pruning, with an explicit EEG read-out
Temporal-sampling / phonological theory (Goswami, 2011)	Atypical low-frequency (δ–θ) auditory sampling underlies dyslexia	Dyslexia	Supplies a candidate *mechanistic cause* (clearance–pruning–TCD) for the very low-frequency anomaly that framework describes at the perceptual level

9. Predictions, falsification, and test strategy

The framework is worth stating because it can be falsified. It predicts: (1) within individuals, clearance efficiency (DTI-ALPS) correlates inversely with delta/theta power and with graph inefficiency; (2) inflammatory load (CSF/serum IL-6, TNF-α; C4b) tracks reduced alpha coordination and disrupted PAC; (3) source-localized abnormality is diffuse in ASD but left-temporoparietal-confined in dyslexia; (4) improving clearance — e.g., sleep optimization — attenuates the low-frequency shift; and (5) ADHD, given already-reduced DTI-ALPS, should show an intermediate, attention-network-weighted variant. Extending the same logic: (6) the low-frequency shift and clearance deficit should *emerge and diverge with age* across the pruning window rather than be fixed from birth; (7) experimental REM/ slow-wave sleep restriction should transiently deepen the theta shift, and sleep optimization attenuate it; (8) vitamin-D status should correlate with signature severity; (9) inflammatory genotype/biomarker load (including APOE and complement-pathway variants) should grade the effect; (10) MEG should reproduce the source-localized spatial dissociation with independent physics; (11) TMS–EEG should reveal altered effective

Received date: July 21 2026
Revised dates;July 22,July 27, Aug,9
Accepted date: Aug. 9 2026

DOI: https://10.63211/j.p.26.204502
ISSN 2760-8646 (Online) ICAITD

connectivity and excitability consistent with the predicted E/I shift; and (12) multimodal convergence — fNIRS/fMRI clearance and perfusion indices and, where ethically justified, PET neuroinflammation markers — should co-vary with the signature within individuals. Predictions (1)–(5) are core; (6)–(12) are progressively more demanding convergent tests. Testing requires what no study has yet done: concurrent multi-domain EEG, lymphatic imaging (DTI-ALPS / dynamic-contrast MRI / NIRS), and immune profiling in a single developmental cohort, analyzed longitudinally and stratified by subtype. Interventional arms (sleep, vitamin D/immunomodulation, glymphatic enhancement) are explicitly hypothesis-generating.

Core versus confirmatory. Not every mechanism carries equal weight, so the model should be tested along its spine first. The minimal, load-bearing chain is: clearance↓ → inflammation↑ → pruning error → reduced effective thalamocortical drive → persistent waking theta. Among the Table 1 features, the single most diagnostic pair is (i) source-localized *waking* theta power and (ii) one graph-topology metric (global efficiency); phase–amplitude coupling, microstates, and entropy are confirmatory refinements. Stating this ordering guards against the "theory that explains everything" failure mode: the framework stands or falls on the core chain, not the accessory features.

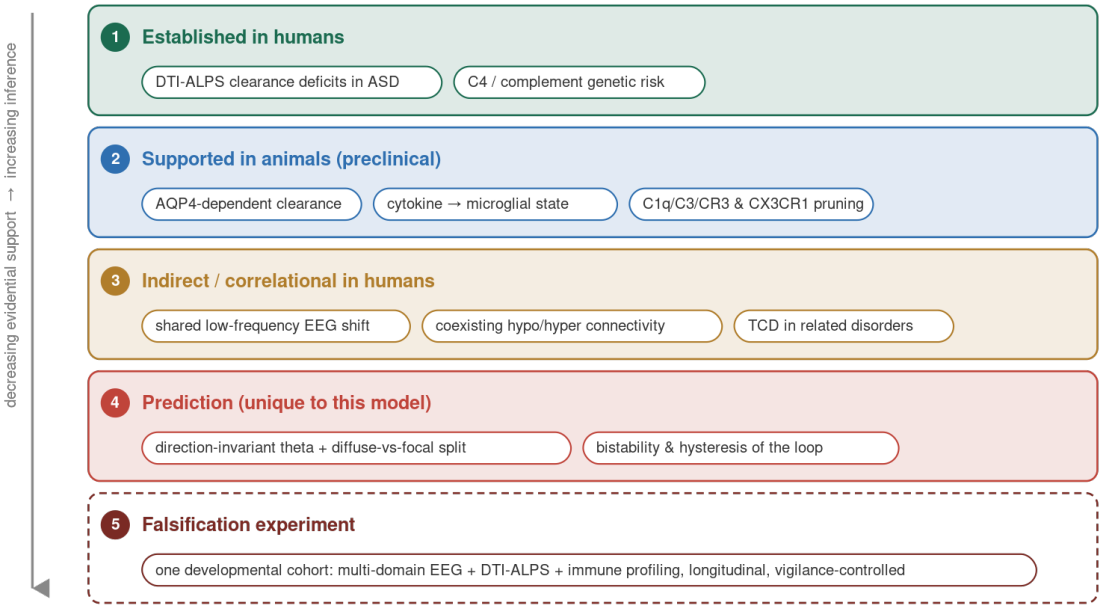

Figure 7. Evidence ladder for the proposed loop. Each claim in the framework is placed at an explicit tier of support, from mechanisms already demonstrated in humans (top) through preclinical and indirect evidence to the model's distinctive predictions and, at the base, the single multimodal experiment that would confirm or refute them. The figure makes the paper's epistemic status legible at a glance: the integrative synthesis rests on well-supported components, whereas the novel, load-bearing steps (the direction-setting bias and the diffuse-versus-focal dissociation) sit at the prediction tier and are the explicit targets of falsification.

Received date: July 21 2026
Revised dates;July 22,July 27, Aug,9
Accepted date: Aug. 9 2026

DOI: https://10.63211/j.p.26.204502
ISSN 2760-8646 (Online) ICAITD

Box 1 — What would falsify this model?

The framework is designed to be disconfirmable. Any of the following results would refute it or a core component:

1. Within individuals, clearance efficiency (DTI-ALPS) shows *no* inverse relationship with waking theta power or graph inefficiency.
2. The theta elevation disappears once arousal and vigilance are controlled — i.e., it is ordinary drowsiness slowing rather than a persistent waking (TCD) rhythm.
3. Source-localized abnormality is *focal* in ASD or *diffuse* in dyslexia, contradicting the spatial-extent axis.
4. Complement-biased (predicted hypoconnective) cases present with hyperconnectivity, or fractalkine-biased cases with frank hypoconnectivity — refuting the direction axis.
5. Sustained improvement of clearance (e.g., durable sleep normalization) leaves the low-frequency shift unchanged over development, contradicting the causal claim.
6. Longitudinally, crossing a clearance threshold fails to produce a *persistent* (hysteretic) theta elevation, refuting the bistability prediction of Figure 5.

10. Future validation and clinical outlook

The steps below are deliberately framed as *future validation targets* rather than clinical recommendations; each presumes that the core loop and its EEG signature first survive the tests of Section 9 and Box 1. Only after that would the following non-invasive, developmentally-timed workflow become worth pursuing.

If even partially validated, the payoff is a non-invasive, developmentally-timed workflow. *Potential stratification:* a composite index combining a multi-domain EEG score, a DTI-ALPS clearance score, and a cytokine panel could separate complement-biased (hypoconnective) from fractalkine-biased (hyperconnective) endophenotypes rather than relying on behavior alone. *Potential prognostic use:* because the model is bistable, early loop markers might flag children at risk of settling into the chronic attractor, defining a treatment window. *Potential monitoring use:* EEG network features are cheap and repeatable, suited to tracking response. *Potential intervention (staged, exploratory):* tier 1, sleep and circadian optimization to raise clearance; tier 2, targeted immunomodulation or vitamin D repletion to reset the microglial set-point; tier 3, mechanism-matched trials guided by endophenotype. None of this is established therapy; it is the clinical shape the hypothesis would take if confirmed.

11. Limitations

The evidence remains predominantly correlational and heavily preclinical. Pruning models differ in region, developmental window, and genetic background; human developmental methods for glymphatic/meningeal function are immature and pediatric biomarkers unvalidated; EEG findings vary with age, subtype, and comorbidity. The systems model, though now simulated and analyzed (bistability, hysteresis, and a saddle-node bifurcation robust across cooperativity), remains *phenomenological*: its parameters capture switch-like

Received date: July 21 2026
Revised dates;July 22,July 27, Aug,9
Accepted date: Aug. 9 2026

DOI: https://10.63211/j.p.26.204502
ISSN 2760-8646 (Online) ICAITD

dynamics rather than measured biological rate constants, so it shows that a loop of this form *can* behave this way, not that the brain *does*. It should be read as a scaffold for experiments, and large effect sizes should not be mistaken for mechanistic proof.

Scope — what this framework does not claim to explain. To avoid a "theory of everything," I state the boundaries plainly. The model addresses one conjunction: a shared, direction-invariant low-frequency (theta) EEG shift together with a diffuse-versus-focal spatial dissociation across ASD and dyslexia. It does *not* explain the full symptom profile of either condition, their genetics or heterogeneity, ADHD or sleep phenotypes except where they touch the clearance–pruning loop, or EEG findings unrelated to low-frequency network organization. The additional measures discussed (phase-amplitude coupling, microstates, entropy, graph metrics) are *confirmatory* tests of the same core mechanism, not separate phenomena the theory independently accounts for. This narrowing is deliberate: a hypothesis is more falsifiable, and more useful, when it declares what lies outside it.

12. Conclusion

Treating microglial pruning and central clearance as one coupled, bistable system — rather than two literatures — yields a compact, falsifiable account of why ASD and dyslexia share a low-frequency EEG shift yet differ in its spatial reach. Its sharpest test is the phenomenon it alone ties together: E/I imbalance, thalamocortical dysrhythmia, complement over-pruning, and temporal-sampling accounts each capture a piece, but none predicts, from a single mechanism, that ASD and dyslexia should share a direction-invariant low-frequency EEG shift *while* dissociating along a diffuse-versus-focal spatial axis. By specifying the molecular pathway, a biophysical reason for the theta shift, a region-specific dyslexia mechanism, a network read-out, and a staged path toward validation, the framework converts scattered correlations into testable predictions and the longitudinal, multimodal design that could confirm or refute them.

References

Abnormal glymphatic system function in children with autism spectrum disorder: a diffusion kurtosis imaging study. (2025). *European Journal of Pediatrics.* https://link.springer.com/article/10.1007/s00431-025-06246-x

Berman, R. A., Gotts, S. J., McAdams, H. M., et al. (2016). Disrupted sensorimotor and social–cognitive networks underlie symptoms in childhood-onset schizophrenia. *Brain, 139*(1), 276–291.

Bosl, W. J., Tierney, A. L., Tager-Flusberg, H., & Nelson, C. A. (2011). EEG complexity as a biomarker for autism spectrum disorder risk. *BMC Medicine, 9*, 18.

Developmental dyslexia: Insights from EEG-based findings and molecular signatures — a pilot study. (2024). *Brain Sciences, 14*(2), 139.

Dynamic local graph-theory indicators based on EEG for diagnosis of autism spectrum disorder. (2024). *Journal of Integrative Neuroscience, 23*(5), 95.

Received date: July 21 2026
Revised dates;July 22,July 27, Aug,9
Accepted date: Aug. 9 2026

DOI: https://10.63211/j.p.26.204502
ISSN 2760-8646 (Online) ICAITD

EEG-based neuroinflammation diagnosis and its role in learning disabilities. (2025). *Diagnostics, 15*(6), 764.

Endogenous retrovirus-derived RNA–DNA hybrids and neuronal C4b induce microglial synaptic pruning in autism models. (2026). *Neuron.* [SETDB1/C4b study]

Estes, M. L., & McAllister, A. K. (2015). Immune mediators in the brain and the pathogenesis of neurodevelopmental disorders. *Nature Reviews Neuroscience, 16*(7), 469–486.

Explainable AI uncovers novel EEG microstate candidate neurophysiological markers for autism spectrum disorder. (2026). *Frontiers in Computational Neuroscience.*

Gabrieli, J. D. E. (2009). Dyslexia: A new synergy between education and cognitive neuroscience. *Science, 325*(5938), 280–283.

Iliff, J. J., & Nedergaard, M. (2013). Is there a cerebral lymphatic system? *Stroke, 44*(6 Suppl 1), S93–S95.

Impaired glymphatic system function and its association with speech and language delay in children with ADHD: a prospective study. (2025). *Frontiers in Human Neuroscience, 19*, 1612997.

Larrain-Valenzuela, J., Zamorano, F., Soto-Icaza, P., et al. (2017). Theta and alpha oscillation impairments reflect working memory deficit. *Scientific Reports, 7*, 14328.

Li, X., et al. (2024). Glymphatic imaging in pediatrics. *Journal of Magnetic Resonance Imaging.* https://doi.org/10.1002/jmri.29040

Llinás, R. R., Ribary, U., Jeanmonod, D., Kronberg, E., & Mitra, P. P. (1999). Thalamocortical dysrhythmia: A neurological and neuropsychiatric syndrome characterized by magnetoencephalography. *PNAS, 96*(26), 15222–15227.

Meng, J., Zhang, L., & Zhang, Y.-w. (2024). Microglial dysfunction in autism spectrum disorder. *The Neuroscientist.* https://doi.org/10.1177/10738584241252576

Multidimensional functional connectivity architecture in preschool children with autism spectrum disorder. (2026). *Brain Sciences, 16*(1), 91.

Over-pruning of synapses in autism-associated SCN2A-deficient mice and human cerebral organoids. (2024). *Molecular Psychiatry.* https://doi.org/10.1038/s41380-024-02518-4

Goswami, U. (2011). A temporal sampling framework for developmental dyslexia. *Trends in Cognitive Sciences, 15*(1), 3–10.

Paolicelli, R. C., & Ferretti, M. T. (2017). Function and dysfunction of microglia during brain development. *Frontiers in Synaptic Neuroscience, 9*, 9.

Rubenstein, J. L. R., & Merzenich, M. M. (2003). Model of autism: increased ratio of excitation/inhibition in key neural systems. *Genes, Brain and Behavior, 2*(5), 255–267.

Received date: July 21 2026
Revised dates;July 22,July 27, Aug,9
Accepted date: Aug. 9 2026

DOI: https://10.63211/j.p.26.204502
ISSN 2760-8646 (Online) ICAITD

Sekar, A., Bialas, A. R., de Rivera, H., et al. (2016). Schizophrenia risk from complex variation of complement component 4. *Nature, 530*(7589), 177–183.

Rasmussen, M. K., Mestre, H., & Nedergaard, M. (2018). The glymphatic pathway in neurological disorders. *The Lancet Neurology, 17*(11), 1016–1024.

The fluidic connectome in brain disease: integrating aquaporin-4 polarity with multisystem pathways. (2025). *International Journal of Molecular Sciences, 26*(23), 11536.

Zhan, Y., Paolicelli, R. C., Sforazzini, F., et al. (2014). Deficient neuron–microglia signaling results in impaired functional brain connectivity and social behavior. *Nature Neuroscience, 17*(3), 400–406.

Received date: July 21 2026
Revised dates;July 22,July 27, Aug,9
Accepted date: Aug. 9 2026

DOI: https://10.63211/j.p.26.204502
ISSN 2760-8646 (Online) ICAITD